Complete $O(\alpha_s^3)$ results for $e^+e^- \to (\gamma, Z) \to$ four jets

Lance Dixon and Adrian Signer

Stanford Linear Accelerator Center, Stanford University, Stanford, California 94309

We present the next-to-leading-order [$O(\alpha_s^3)$] perturbative QCD predictions for e^+e^- annihilation into four jets. A previous calculation omitted the $O(\alpha_s^3)$ terms suppressed by one or more powers of $1/N_c^2$, where N_c is the number of colors, and the ''light-by-glue scattering'' contributions. We find that all such terms are uniformly small, constituting less than 10% of the correction. For the Durham clustering algorithm, the leading and next-to-leading logarithms in the limit of the small jet resolution parameter y_{cut} can be resummed. We match the resummed results to our fixed-order calculation in order to improve the small y_{cut} prediction. [S0556-2821(97)05719-6]

I. INTRODUCTION

Electron-positron annihilation into jets provides an arena for studying quantum chromodynamics (QCD) that is free of initial-state uncertainties such as parton distribution functions. At the large center-of-mass energies achieved by the SLAC Linear Collider (SLC), CERN e^+e^- collider LEP, and now LEP 2, e^+e^- annihilation is also relatively free of nonperturbative final-state effects, i.e., hadronization corrections. On the other hand, perturbative QCD corrections to jet rates can be very large. For example, the three-jet rate at the Z^0 pole receives a 20–30 % correction [1] at order α_s^2. These next-to-leading-order (NLO) corrections are of course critical for obtaining a precise experimental measurement of α_s from the three-jet rate and related $O(\alpha_s)$ observables [2,3].

More recently, the NLO corrections to e^+e^- production of four jets were computed, and a correction of roughly 100% was found [4] for most jet algorithms (when the renormalization scale was set equal to the center-of-mass energy). This computation omitted terms suppressed by one or more powers of $1/N_c^2$, where N_c is the number of colors in a general SU(N_c) gauge theory ($N_c = 3$ for QCD). It also neglected the ''light-by-glue scattering'' contributions — interference terms where two different flavor quarks couple to the virtual photon or Z boson. In this work we present the complete $O(\alpha_s^3)$ results, using an improved version of the same numerical program, MENLO_PARC [5], which was employed for the leading-in-N_c computation. The crucial ingredients for the construction of the program are the tree-level amplitudes for five massless final-state partons, $e^+e^- \to q\bar{q}ggg$ and $e^+e^- \to q\bar{q}q'\bar{q}'g$ [6,7], and especially the recently computed one-loop virtual amplitudes for $e^+e^- \to q\bar{q}q'\bar{q}'$ [8,9] and $e^+e^- \to q\bar{q}gg$ [10]. We use the formulas given in [6,9,10].

The NLO prediction of the four-jet fraction — an observable whose expansion begins at order α_s^2 — makes it possible to measure $\alpha_s^{\overline{\text{MS}}}$ with the same formal level of precision (NLO) as has previously been reserved for $O(\alpha_s)$ observables in e^+e^- annihilation. However, the theoretical uncertainty in such a measurement will still be sizable: Because the one-loop corrections are so large, the renormalization-scale dependence of the NLO four-jet result is still strong, and it is likely that uncalculated higher-order corrections are important. Also, a significant four-jet rate only appears at smaller values of the jet resolution parameter y_{cut}, where there are large perturbative logarithms, although these can be partially resummed for the Durham algorithm [11].

There are at least two other motivations for studying e^+e^- annihilation to four jets: (1) These events are a background to $e^+e^- \to W^+W^- \to 4$ jets, particularly when the center-of-mass energy is not far above the W-pair threshold, as is the case at LEP 2. (2) Four-jet final states provide QCD tests to which three-jet events are insensitive [12]. For example, the non-Abelian three-gluon vertex appears at leading order in four-jet events; the same is true for the production of hypothetical, light, colored but electrically neutral particles, such as light gluinos [13–16]. In both applications, distributions of the four jets with respect to energies and angles [12] are important. Such distributions can be computed at NLO using the same numerical program, and will be the subject of a separate publication [17]; here we briefly study the sensitivity of the total four-jet rate to additional light fermions.

The remainder of the paper is organized as follows. In Sec. II we describe the dependence of the four-jet rate on electroweak and color factors, and outline the structure of the numerical calculation. In Sec. III we present the complete $O(\alpha_s^3)$ predictions for three different jet algorithms. We indicate the dependence of the predictions on the (unphysical) renormalization scale μ. The Geneva algorithm [18] has a relatively mild μ dependence (small NLO correction) and a relatively strong dependence on the number of light quark flavors N_f; we discuss the extent to which N_f can be determined from the Geneva four-jet rate alone. In Sec. IV we present results from matching the resummed Durham jet rate to the fixed-order $O(\alpha_s^3)$ results; the improved prediction agrees quite well with preliminary SLD data [19]. Section V contains our conclusions.

II. STRUCTURE OF THE CROSS SECTION AND COMPUTATION

For computational reasons as well as to study the effect of varying parameters, it is useful to decompose the leading-

order (Born) and NLO contributions to the four-jet differential cross section with respect to both their electroweak and QCD (color) structure. To simplify the electroweak decomposition we assume that the observable being calculated is insensitive to both (1) correlations between the final-state hadrons and the electron-positron beam direction, and (2) quark and gluon helicities. We also assume the positrons are unpolarized and the electrons have a longitudinal polarization of P_e ($P_e = +1$ for a right-handed beam). QED initial-state radiation and other electroweak corrections are neglected. Then the helicity-summed four-jet (differential) cross section at center-of-mass energy $\sqrt{s}$ may be written

$$\sigma_{\text{four-jet}} = \frac{4\pi\alpha^2}{3s} N_c [f^{(\text{I})}(s)\sigma_4^{(\text{I})} + f^{(\text{II})}(s)\sigma_4^{(\text{II})} + f^{(\text{III})}(s)\sigma_4^{(\text{III})}], \tag{1}$$

where

$$f^{(\text{I})}(s) = \sum_q (Q^q)^2 + \frac{1}{4}[(v_L^e)^2(1-P_e)+(v_R^e)^2(1+P_e)]\sum_q [(v_L^q)^2+(v_R^q)^2]|\mathcal{P}_Z(s)|^2$$

$$- \frac{1}{2}[v_L^e(1-P_e)+v_R^e(1+P_e)]\left(\sum_q Q^q(v_L^q+v_R^q)\right)\text{Re}\mathcal{P}_Z(s),$$

$$f^{(\text{II})}(s) = \left(\sum_q Q^q\right)^2 + \frac{1}{8}[(v_L^e)^2(1-P_e)+(v_R^e)^2(1+P_e)]\left(\sum_q (v_L^q+v_R^q)\right)^2|\mathcal{P}_Z(s)|^2$$

$$- \frac{1}{2}[v_L^e(1-P_e)+v_R^e(1+P_e)]\left(\sum_q Q^q\right)\left(\sum_q (v_L^q+v_R^q)\right)\text{Re}\mathcal{P}_Z(s),$$

$$f^{(\text{III})}(s) = \frac{1}{8\sin^2 2\theta_W}[(v_L^e)^2(1-P_e)+(v_R^e)^2(1+P_e)]|\mathcal{P}_Z(s)|^2, \tag{2}$$

where α is the fine structure constant, Q^q is the charge of quark q in units of e, and the left- and right-handed couplings to the Z^0 are

$$v_L^e = \frac{-1+2\sin^2\theta_W}{\sin 2\theta_W}, \quad v_R^e = \frac{2\sin^2\theta_W}{\sin 2\theta_W},$$

$$v_L^q = \frac{\pm 1 - 2Q^q\sin^2\theta_W}{\sin 2\theta_W}, \quad v_R^q = -\frac{2Q^q\sin^2\theta_W}{\sin 2\theta_W}, \tag{3}$$

where θ_W is the weak mixing angle; the two signs in v_L^q correspond to up ($+$) and down ($-$) type quarks. Equations (1) and (2) include both virtual photon and Z boson exchange (and their interference); the ratio of Z and photon propagators is given by

$$\mathcal{P}_Z(s) = \frac{s}{s-M_Z^2+i\Gamma_Z M_Z}, \tag{4}$$

where M_Z and Γ_Z are the mass and width of the Z.

Representatives of the classes of diagrams contributing to $f^{(\text{I})}$, $f^{(\text{II})}$, and $f^{(\text{III})}$ are depicted in Fig. 1 as amplitude interferences. Five-parton cuts of these graphs, shown as dashed lines, correspond to the real part of the NLO correction; four-parton cuts, shown as dotted lines, correspond to the virtual part. In contribution (I) a single fermion couples to both (γ,Z) vector bosons in the interference, via either a vector or axial vector coupling. (As shown in the figure, there may be a second or even a third fermion loop in the interior of the graph, corresponding to "QCD" factors of N_f in the cross section.) This contribution dominates the cross section at $O(\alpha_s^2)$ and as we will see, again at $O(\alpha_s^3)$.

The remaining contributions, (II) and (III), have different origins in the real and virtual parts of the calculation. In the real part they come from the $q\bar{q}q'\bar{q}'g$ final state when the roles of q and q' are exchanged on the opposite side of the cut; in particular, a different quark pair couples to the (γ,Z) on each side of the interference. In the virtual part they can
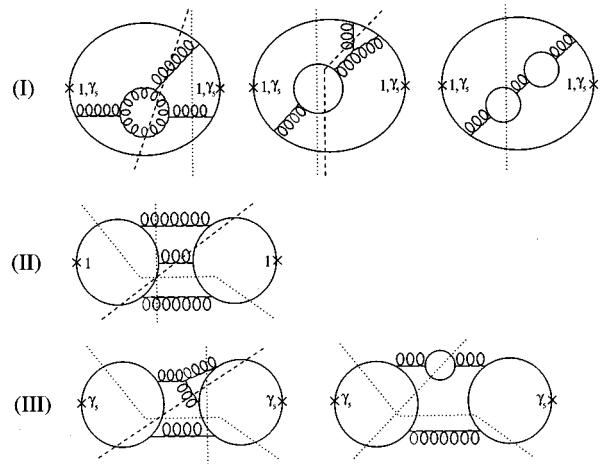

FIG. 1. Representative contributions of types (I), (II), and (III), as described in the text. The coupling of a quark to the (γ,Z) vector boson is denoted by $\times$, with a 1 (γ_5) for vector (axial vector) coupling. Dashed lines correspond to representative five-parton cuts; dotted lines to four-parton cuts.

have the same kind of exchange origin in $q\bar{q}q'\bar{q}'$ final states, but they can also arise from either $q\bar{q}gg$ or $q\bar{q}q'\bar{q}'$ graphs where a quark loop couples directly to the photon or Z (for example, the contribution $A_{6;3}$ (A_6^{ax}) in [9]).

Contribution (II) represents ''light-by-glue scattering,'' whereby a different fermion line couples to each vector boson, via a vector coupling in each case. There is no such contribution at $O(\alpha_s^2)$ if only charge-blind observables are considered [20], due to Furry's theorem — the order α_s^2 amplitude interferences all contain fermion triangle subgraphs. Although the cross section is nonvanishing at $O(\alpha_s^3)$, we shall see that it is still extremely small, due partly to cancellations in the sum over quark couplings in $f^{(II)}(s)$, and partly to approximate cancellations in the phase-space integrations that are related to the exact cancellations at order α_s^2.

Contribution (III), ''Z-by-glue'' scattering, is similar to contribution (II) except that the quarks couple to the Z through the axial vector coupling. This contribution is non-zero at $O(\alpha_s^2)$ [21], although small for the three- and four-jet rates, and it remains small at $O(\alpha_s^3)$. In Eq. (2) we have already carried out the sum over the five light quark flavors, in which the massless weak isospin doublets (u,d) and (c,s) cancelled, leaving only the (t,b) contribution. The top quark contribution to (III) is purely virtual for $\sqrt{s} < 2m_t$, but it does not decouple in the large m_t limit [21]. We expand in the limit of large top quark mass, including all terms through $O(s/m_t^2)$; at this order the top quark does not appear in the vector contribution (II) [9,10].

Dividing the four-jet cross section $\sigma_{\text{four-jet}}$ by the total hadronic cross section at $O(\alpha_s)$,

$$\sigma_{\text{tot}} = \frac{4\pi\alpha^2}{3s} N_c f^{(I)}(s)\left(1 + \frac{\alpha_s}{\pi}\right), \qquad (5)$$

yields the four-jet fraction

$$R_4 \equiv \frac{\sigma_{\text{four-jet}}}{\sigma_{\text{tot}}} = \left[\sigma_4^{(I)} + \frac{f^{(II)}}{f^{(I)}}\sigma_4^{(II)} + \frac{f^{(III)}}{f^{(I)}}\sigma_4^{(III)}\right]\left(1 + \frac{\alpha_s}{\pi}\right)^{-1}. \qquad (6)$$

Neglecting for the moment the renormalization-scale dependence of the calculated cross section we write the expansion in α_s as

$$R_4 = \left[\left(\frac{\alpha_s}{2\pi}\right)^2 B_4 + \left(\frac{\alpha_s}{2\pi}\right)^3 C_4\right]\left(1 + \frac{\alpha_s}{\pi}\right)^{-1}, \qquad (7)$$

$$\frac{f^{(A)}}{f^{(I)}}\sigma_4^{(A)} = \left(\frac{\alpha_s}{2\pi}\right)^2 B_4^{(A)} + \left(\frac{\alpha_s}{2\pi}\right)^3 C_4^{(A)}, \quad A = \text{I,II,III}, \quad (8)$$

Next we decompose the one-loop correction to $\sigma_4^{(I)}$ with respect to N_c and N_f:

$$C_4^{(I)} = N_c^2(N_c^2 - 1)\left[\sigma_4^{(a)} + \frac{N_f}{N_c}\sigma_4^{(b)} + \frac{N_f^2}{N_c^2}\sigma_4^{(c)} + \frac{1}{N_c^2}\sigma_4^{(d)}\right.$$
$$\left. + \frac{N_f}{N_c^3}\sigma_4^{(e)} + \frac{1}{N_c^4}\sigma_4^{(f)}\right]. \qquad (9)$$

Correspondingly, we write the full $O(\alpha_s^3)$ correction to the four-jet rate as

$$C_4 = C_4^{(a)} + C_4^{(b)} + C_4^{(c)} + C_4^{(d)} + C_4^{(e)} + C_4^{(f)} + C_4^{(II)} + C_4^{(III)}, \qquad (10)$$

absorbing all prefactors into the definitions of the $C_4^{(x)}$. In [4] we calculated $C_4^{(a,b,c)}$; here we add the remaining terms in Eq. (10). The subleading-color terms $C_4^{(d,e,f)}$ come partly from nonplanar interference graphs (not shown in Fig. 1). They include identical-quark Pauli exchange contributions analogous to the E terms of [20], as well as various subleading-color virtual subamplitudes [9,10], and subleading terms in the real and virtual color sums. We find that all the additional terms are considerably smaller than $C_4^{(a,b,c)}$, at least for the overall four-jet rate.

The Monte Carlo integrations required to numerically evaluate the $C_4^{(x)}$ are done separately for each term, except that $C_4^{(d)}$ and $C_4^{(f)}$ are combined. An advantage [4] of breaking up the problem in this way is that the $1/N_c^2$-suppressed integrands have significantly more complicated analytic representations than the leading terms, and therefore take more time per point to evaluate (in some cases up to a factor of 5 longer). On the other hand, the $1/N_c^2$ parametric suppression implies that far fewer numerical evaluations of the subleading terms are required in order to achieve an absolute statistical accuracy comparable to that for the leading-in-N_c terms. Contributions (II) and (III) could have been further decomposed by analogy to Eq. (9), but in view of their small overall contribution they were each integrated as a single expression.

As in any NLO QCD computation, the real and virtual corrections to the cross section are separately divergent, but have a finite sum. In dimensional regularization with $D = 4 - 2\epsilon$, the singularities of the virtual part manifest themselves as poles in ϵ in the one-loop amplitudes, whereas the real singularities are obtained upon phase-space integration of the squared tree amplitudes. We use a general version of the subtraction method [20] to extract the singular parts of the real cross section and combine them with the virtual poles. This method leaves a finite integral over five-parton phase space, and another over four-parton phase space, which are performed by adaptive Monte Carlo integration using VEGAS [22]. The particular form of the subtraction method used here is essentially that described in [23], to which we refer the reader for more details. No approximation of the matrix elements or the phase space has to be made in this method.

The subtraction method relies on the fact that the integral over the tree cross section is rendered finite by subtracting all soft and collinear limits. This means that for a phase-space point that lies very close to a singular point, the integrand is the square of the difference of two large numbers, namely the tree amplitude and its soft or collinear limit. In order to obtain the desired cancellation it is crucial to compute this difference in a numerically stable way, even if a certain invariant mass becomes very small. Thus, if the phase-space point is so close to a singular point that a straightforward evaluation of the amplitude becomes unstable, the amplitude is replaced by its (more stable) soft or collinear limit. We

checked that the error introduced by this treatment is completely negligible. We also checked that our results are independent of the arbitrary parameters δ and ξ_{cut} which have to be introduced in the subtraction method [23].

Another potential numerical problem is related to spurious singularities in the one-loop amplitudes. Besides the expected poles in the soft and collinear limits (which are avoided by the program since they lie in the three-jet region), the one-loop amplitudes have unphysical poles, i.e., poles with zero residue. Unfortunately, it is not possible to eliminate all these poles analytically, as long as the amplitude is expressed in terms of logarithms and dilogarithms multiplied by kinematic coefficients [10]; this elimination is only possible if the amplitude is rewritten in terms of more general functions [24]. However, in the helicity formalism, one can simplify the (di)logarithmic coefficients to greatly alleviate the spurious poles [10]. We checked that the numerical evaluation of the matrix elements as given in [9,10] is stable, even for points that are quite close to a spurious pole, and that the probability for hitting an unstable point in the Monte Carlo integration is very small. Indeed, we had to evaluate close to a million points in a test run (corresponding to subpercent statistical accuracy on the integral) in order to find one point that was ''close'' to a particular spurious pole; at that one point the value of the vanishing denominator was still about an order of magnitude larger than where the numerical evaluation of the cross section typically becomes unstable.

III. FIXED-ORDER RESULTS

We now present results for the four-jet fraction R_4 at next-to-leading order in α_s. We use $N_c = 3$ colors, $N_f = 5$ massless quarks, a strong coupling constant of $\alpha_s(M_Z) = 0.118$, a top mass of $m_t = 175$ GeV, a Z^0 mass and width of $M_Z = 91.187$ GeV and $\Gamma_Z = 2.490$ GeV, and a weak mixing angle of $\sin^2\theta_W = 0.230$ [25]. The numerical results given here are for $\sqrt{s} = M_Z$, but to the extent that contributions (II) and (III) can be neglected, R_4 depends essentially only on N_c, N_f, and $\alpha_s(\sqrt{s})$. We consider the E0, Durham [26,11], and Geneva [18] jet algorithms. These cluster algorithms begin with a set of final-state particles (partons in the QCD calculation) and cluster the pair $\{i,j\}$ with the smallest value of a dimensionless measure y_{ij} into a single ''protojet.'' The procedure is repeated until all the y_{ij} exceed the value of the jet resolution parameter y_{cut}, at which point the protojets are declared to be jets. The algorithms differ in the measure y_{ij} used and/or in the rule used to assign a four-momentum p_{ij} to two clustered momenta p_i, p_j. The same value of y_{cut} in different schemes may sample quite different classes of events. For the reader's convenience, we collect the definitions of the E0, Durham, and Geneva schemes in Table I.

We start the presentation of the results with the E0 scheme. Figure 2(a) shows the absolute value of the contributions of the different electroweak/color pieces to the four-jet fraction at $\sqrt{s} = M_Z$, as a function of y_{cut}, setting the renormalization scale to $\mu = M_Z$. Note (from Table II) that $C_4^{(b)} + C_4^{(c)}$, $C_4^{(d)} + C_4^{(f)}$ and $C_4^{(III)}$ are negative. These curves are compared to preliminary SLAC Large Detector (SLD) data points [19] which have been corrected for detector ef-

TABLE I. Jet algorithm definitions.

Algorithm	y_{ij}	p_{ij}
E0	$\dfrac{(p_i+p_j)^2}{s}$	$(E_i+E_j)\left(1, \dfrac{\vec{p}_i+\vec{p}_j}{\|\vec{p}_i+\vec{p}_j\|}\right)$
Durham	$2\min(E_i^2, E_j^2)\dfrac{1-\cos\theta_{ij}}{s}$	p_i+p_j
Geneva	$\dfrac{8}{9}E_iE_j\dfrac{1-\cos\theta_{ij}}{(E_i+E_j)^2}$	p_i+p_j

fects and hadronization. Obviously the comparison would benefit from a reanalysis using the full current Z^0 pole data samples. As expected, the subleading-color pieces are roughly 10% of the corresponding leading-color contributions, reflecting the $1/N_c^2$ suppression. This feature holds separately for the terms lacking and having an N_f factor. The contributions (II) and (III) are so small that we multiply them by a factor of 1000 and 10, respectively, in the figure. Table II presents the same results, for $y_{cut} \in \{0.005, 0.01, 0.03\}$, namely the coefficients $(\alpha_s/2\pi)^3 C_4^{(x)}/(1+\alpha_s/\pi)$ at $\sqrt{s} = M_Z$, including the statistical uncertainties from Monte Carlo integration. The ''Born'' line gives the tree-level result $(\alpha_s/2\pi)^2 B_4/(1+\alpha_s/\pi)$.

Observable quantities calculated in QCD should be independent of the arbitrary renormalization scale μ. However, the perturbative expansion is invariably truncated at a finite order, leading to a residual dependence of the result on μ. The tree-level μ dependence is much stronger for the four-jet rate than for the three-jet rate, because the former is proportional to α_s^2 instead of α_s. The full μ dependence of the NLO four-jet rate is given by
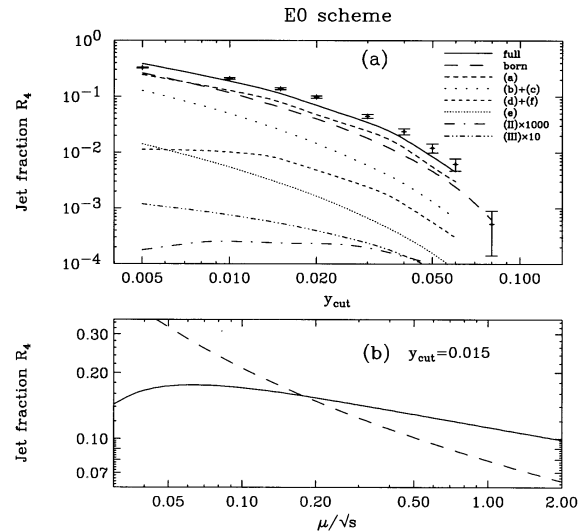

FIG. 2. (a) Absolute value of the contributions of the different electroweak-color pieces to the four-jet fraction at $\sqrt{s} = M_Z$ for the E0 scheme, i.e., $(\alpha_s/2\pi)^3|C_4^{(x)}|/(1+\alpha_s/\pi)$ with $x \in \{a,b,c,d,e,f,II,III\}$. We also show the Born and full one-loop prediction, and data from [19]. (b) Dependence of the tree-level (dashed line) and one-loop (solid line) prediction on the renormalization scale μ for $y_{cut} = 0.015$.

TABLE II. E0 algorithm.

Contribution to R_4	$y_{cut}=0.005$	$y_{cut}=0.01$	$y_{cut}=0.03$
Born	$(2.60\pm0.02)\times10^{-1}$	$(1.16\pm0.01)\times10^{-1}$	$(1.79\pm0.01)\times10^{-2}$
a	$(2.43\pm0.08)\times10^{-1}$	$(1.27\pm0.03)\times10^{-1}$	$(2.42\pm0.05)\times10^{-2}$
b	$-(1.23\pm0.02)\times10^{-1}$	$-(4.75\pm0.04)\times10^{-2}$	$-(5.57\pm0.06)\times10^{-3}$
c	$-(4.06\pm0.02)\times10^{-3}$	$-(1.83\pm0.01)\times10^{-3}$	$-(2.93\pm0.01)\times10^{-4}$
$d+f$	$-(1.13\pm0.18)\times10^{-2}$	$-(1.01\pm0.08)\times10^{-2}$	$-(2.42\pm0.10)\times10^{-3}$
e	$(1.42\pm0.01)\times10^{-2}$	$(5.45\pm0.04)\times10^{-3}$	$(6.69\pm0.06)\times10^{-4}$
II	$(1.66\pm0.28)\times10^{-7}$	$(2.43\pm0.32)\times10^{-7}$	$(1.88\pm0.18)\times10^{-7}$
III	$-(1.18\pm0.01)\times10^{-4}$	$-(7.53\pm0.03)\times10^{-5}$	$-(2.37\pm0.02)\times10^{-5}$
Full$\equiv R_4$	$(3.79\pm0.08)\times10^{-1}$	$(1.88\pm0.03)\times10^{-1}$	$(3.46\pm0.05)\times10^{-2}$

$$\sigma_4(\mu) = \left(\frac{\alpha_s(\mu)}{2\pi}\right)^2 B_4 + \left(\frac{\alpha_s(\mu)}{2\pi}\right)^3 \left[C_4 + 2\beta_0 \ln\left(\frac{\mu^2}{s}\right)B_4\right],$$
(11)

where $\alpha_s(\mu)$ is the two-loop running coupling,

$$\alpha_s(\mu) = \frac{\alpha_s(M_Z)}{w}\left(1 - \frac{\alpha_s(M_Z)}{\pi}\frac{\beta_1}{\beta_0}\frac{\ln(w)}{w}\right),$$

$$w = 1 - \beta_0\frac{\alpha_s(M_Z)}{\pi}\ln\left(\frac{M_Z}{\mu}\right),$$
(12)

with $\beta_0 = \frac{1}{2}(\frac{11}{3}C_A - \frac{2}{3}N_f)$, $\beta_1 = \frac{1}{4}[\frac{17}{3}C_A^2 - (\frac{5}{3}C_A + C_F)N_f]$, $C_A = N_c$, $C_F = (N_c^2-1)/(2N_c)$. As expected, the strong renormalization-scale dependence of the tree-level result is reduced by the inclusion of the next-to-leading order contribution. Figure 2(b) plots the μ dependence of R_4 at tree level and at one loop for the E0 scheme, at $y_{cut}=0.015$.

The results for the Durham scheme are presented in Table III, for the same values of y_{cut} as in the E0 scheme. Again, the subleading-color terms are of the expected size.

The Geneva algorithm has the feature that the leading-order results, evaluated at $\mu = \sqrt{s}$, give a reasonable description of the data for large values of y_{cut}, although the shape of the prediction is not quite correct, especially at small y_{cut}. Also, the renormalization-scale dependence is quite flat at moderate y_{cut}. Finally, the dependence of the prediction on the number of light flavors N_f is reasonably large, at least in comparison with other algorithms (see Table IV). There is

some interest in experimentally constraining N_f, in particular because a massless gluino would effectively shift the value of N_f by $\Delta N_f = +3$ in $O(\alpha_s^2)$ four-jet distributions [13,14]. [At $O(\alpha_s^3)$ the effect is not simply given by $\Delta N_f = +3$, as is illustrated by the structure of the $O(\alpha_s^3)$ results for the total e^+e^- hadronic cross section [27].] Various authors have suggested that the existence of a light gluino is already in doubt [14,28,16]. Nevertheless, we would like to ask whether one can determine N_f with sufficient accuracy solely from the overall four-jet rate in the Geneva algorithm. In Fig. 3 we plot the NLO Geneva prediction as a function of y_{cut} for $N_f=5$ (u,d,s,c, and b quarks) and $N_f=8$ (u,d,s,c, and b quarks, plus a massless gluino), where the bands represent the variation of μ over the interval $[\frac{1}{2}\sqrt{s}, 2\sqrt{s}]$ and $[\frac{1}{3}\sqrt{s}, 3\sqrt{s}]$, respectively. These bands are compared to preliminary SLD data [19]. The huge uncertainty for small values of y_{cut} reflects the fact that the fixed-order prediction is not converging well for $y_{cut}\lesssim0.02$, presumably due to large logarithms of $1/y_{cut}$. This breakdown happens at larger y_{cut} for $N_f=8$, since in this particular case $C_4^{(b)}$ is the dominant contribution to the one-loop correction, and it is further enhanced if N_f is increased from 5 to 8.

As can be seen in Fig. 3 the data tend to favor $N_f=5$, at least for $0.03\lesssim y_{cut}\lesssim0.04$, however, the uncertainties coming from uncalculated higher-order terms are still too large to permit excluding light gluinos using this observable alone.

Various angular distributions in four-jet events have been proposed to help separate the relatively small contributions

TABLE III. Durham algorithm.

Contribution to R_4	$y_{cut}=0.005$	$y_{cut}=0.01$	$y_{cut}=0.03$
Born	$(6.78\pm0.02)\times10^{-2}$	$(2.87\pm0.01)\times10^{-2}$	$(4.11\pm0.01)\times10^{-3}$
a	$(6.60\pm0.13)\times10^{-2}$	$(3.03\pm0.06)\times10^{-2}$	$(4.23\pm0.07)\times10^{-3}$
b	$-(2.68\pm0.02)\times10^{-2}$	$-(1.03\pm0.01)\times10^{-2}$	$-(1.24\pm0.02)\times10^{-3}$
c	$-(1.27\pm0.01)\times10^{-3}$	$-(5.16\pm0.02)\times10^{-4}$	$-(6.94\pm0.02)\times10^{-5}$
$d+f$	$-(4.54\pm0.41)\times10^{-3}$	$-(2.50\pm0.09)\times10^{-3}$	$-(3.67\pm0.45)\times10^{-4}$
e	$(2.93\pm0.02)\times10^{-3}$	$(1.14\pm0.01)\times10^{-3}$	$(1.43\pm0.01)\times10^{-4}$
II	$(2.28\pm0.20)\times10^{-7}$	$(2.22\pm0.12)\times10^{-7}$	$(9.06\pm0.39)\times10^{-8}$
III	$-(5.57\pm0.03)\times10^{-5}$	$-(3.16\pm0.02)\times10^{-5}$	$-(7.82\pm0.07)\times10^{-6}$
Full$\equiv R_4$	$(1.04\pm0.02)\times10^{-1}$	$(4.70\pm0.06)\times10^{-2}$	$(6.82\pm0.08)\times10^{-3}$

TABLE IV. Geneva algorithm.

Contribution to R_4	$y_{cut}=0.02$	$y_{cut}=0.03$	$y_{cut}=0.05$
Born	$(2.63\pm0.02)\times10^{-1}$	$(1.50\pm0.01)\times10^{-1}$	$(6.33\pm0.02)\times10^{-2}$
a	$(1.16\pm0.05)\times10^{-1}$	$(8.91\pm0.25)\times10^{-2}$	$(4.90\pm0.14)\times10^{-2}$
b	$-(1.37\pm0.02)\times10^{-1}$	$-(6.99\pm0.09)\times10^{-2}$	$-(2.51\pm0.03)\times10^{-2}$
c	$-(7.78\pm0.12)\times10^{-3}$	$-(4.32\pm0.04)\times10^{-3}$	$-(1.68\pm0.02)\times10^{-3}$
$d+f$	$(6.90\pm1.07)\times10^{-3}$	$-(1.10\pm1.88)\times10^{-3}$	$-(2.55\pm0.78)\times10^{-3}$
e	$(1.44\pm0.02)\times10^{-2}$	$(7.58\pm0.08)\times10^{-3}$	$(2.83\pm0.03)\times10^{-3}$
II	$(1.72\pm0.52)\times10^{-7}$	$(2.89\pm0.47)\times10^{-7}$	$(2.53\pm0.35)\times10^{-7}$
III	$-(1.06\pm0.02)\times10^{-4}$	$-(7.86\pm0.06)\times10^{-5}$	$-(4.91\pm0.04)\times10^{-5}$
Full$\equiv R_4$	$(2.56\pm0.06)\times10^{-1}$	$(1.71\pm0.03)\times10^{-1}$	$(8.58\pm0.15)\times10^{-2}$

of four-quark final states from the dominant two-quark two-gluon final states [12]. These distributions have been studied at leading order in α_s in order to constrain N_f as well as the other color factors C_A and C_F [29,15,16]. The next-to-leading-order corrections to the distributions will be discussed elsewhere [17], but they are remarkably small, given the size of the corrections to the overall four-jet rate. Unfortunately, in many cases the dependence on N_f is not that strong, such that a precise determination of N_f is difficult in the face of hadronization uncertainties.

IV. RESUMMED RESULTS

The four-jet fraction declines rapidly at large y_{cut}, and there are little data publicly available with which to compare our predictions for $y_{cut}>0.07$. On the other hand, at the kinematic limit $y_{cut}\to0$ the QCD expansion parameter becomes $\alpha_s L^2$, where $L=\ln(1/y_{cut})$, and the NLO prediction would be improved if these large logarithms could be resummed. This is possible at leading order (LL) and next-to-leading order (NLL) in L in the Durham clustering algorithm because the phase space factorizes appropriately [11]. The NLL four-jet rate is then given by [11]

$$R_4^{NLL}=2[\Delta_q(Q)]^2\Bigg[\Bigg(\int_{Q_0}^{Q}dq\Gamma_q(Q,q)\Delta_g(q)\Bigg)^2$$

$$+\int_{Q_0}^{Q}dq\Gamma_q(Q,q)\Delta_g(q)\int_{Q_0}^{q}dq'[\Gamma_g(q,q')\Delta_g(q')$$

$$+\Gamma_f(q')\Delta_f(q')]\Bigg].\tag{13}$$

The NLL emission probabilities are

$$\Gamma_q(Q,q)=\frac{2C_F}{\pi}\frac{\alpha_s(q)}{q}\Bigg(\ln\frac{Q}{q}-\frac{3}{4}\Bigg),$$

$$\Gamma_g(Q,q)=\frac{2C_A}{\pi}\frac{\alpha_s(q)}{q}\Bigg(\ln\frac{Q}{q}-\frac{11}{12}\Bigg),$$

$$\Gamma_f(q)=\frac{N_f}{3\pi}\frac{\alpha_s(q)}{q},\tag{14}$$

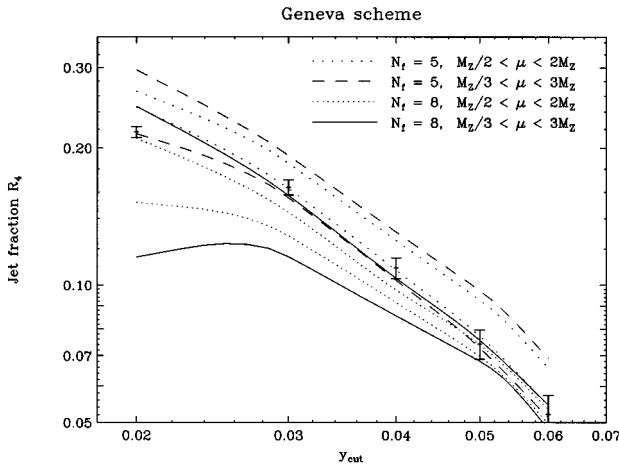and the Sudakov factors (probability of no emission) are

FIG. 3. NLO prediction for the four-jet rate using the Geneva algorithm for $N_f=5$ and $N_f=8$. The theoretical bands have been obtained by varying the renormalization scale from $\frac{1}{2}\sqrt{s}<\mu<2\sqrt{s}$ and from $\frac{1}{3}\sqrt{s}<\mu<3\sqrt{s}$. The data are from [19].
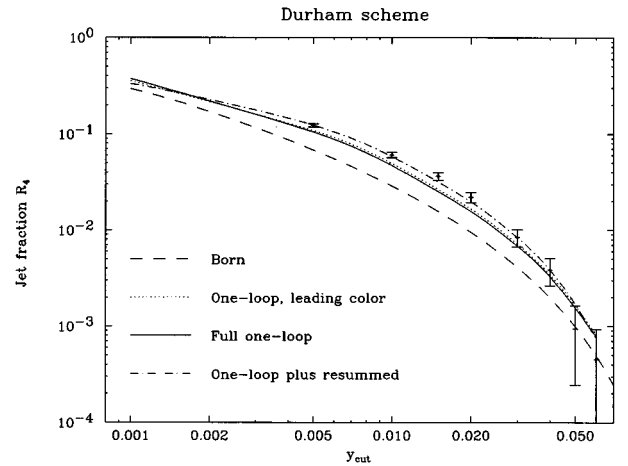

FIG. 4. The four-jet fraction for the Durham algorithm at $\sqrt{s}=M_Z$, illustrating the improvements to the Born term from adding successively the leading-color loop corrections, the subleading-color corrections, and the resummed corrections after matching. The data are from [19].

$$\Delta_q(Q) = \exp\left(-\int_{Q_0}^Q dq\, \Gamma_q(Q,q)\right),$$

$$\Delta_g(Q) = \exp\left(-\int_{Q_0}^Q dq[\Gamma_q(Q,q)+\Gamma_f(q)]\right),$$

$$\Delta_f(Q) = \frac{[\Delta_q(Q)]^2}{\Delta_g(Q)}. \tag{15}$$

The Durham four-jet rate is an example of a quantity that can be resummed at leading and next-to-leading logarithmic order, but which does not exponentiate. The NLL results for such quantities do not include the proper renormalization-scale dependence of even the leading-log terms [30]: Under a change of renormalization scale, a leading term $\alpha_s^n L^{2n}$ varies by $\sim \alpha_s^{n+1} L^{2n} = \alpha_s^{n+1} L^{2(n+1)-2}$, which is not contained in the NLL approximation. This is reflected in a relatively large ''scale uncertainty.'' Thus one should not rely on the resummed R_4 alone for a determination of $\alpha_s^{\overline{\text{MS}}}$.

Indeed at finite values of y_{cut} one should match the resummed results with the fixed-order results. For observables that exponentiate, a number of matching schemes have been defined [31,3]—R matching, $\ln R$ matching, modified R matching, and modified $\ln R$ matching. For R_4, the following matching scheme corresponds to R matching:

$$R_4^{R\text{ match}} = R_4^{\text{NLL}} + \left[\left(\frac{\alpha_s}{2\pi}\right)^2 (B_4 - B_4^{\text{NLL}}) + \left(\frac{\alpha_s}{2\pi}\right)^3 (C_4 - C_4^{\text{NLL}})\right]$$
$$\times \left(1 + \frac{\alpha_s}{\pi}\right)^{-1}, \tag{16}$$

where the ''overlap'' terms B_4^{NLL} and C_4^{NLL} are defined by expanding R_4^{NLL} out in powers of α_s, in analogy to Eq. (7). A modified R-matching scheme could be defined by replacing $L = \ln(1/y_{\text{cut}})$ by $\ln(y_{\text{cut}}^{-1} - y_{\text{max}}^{-1} + 1)$ in R_4^{NLL}, where y_{max} is the maximum kinematic value of y_{cut}. This scheme would switch the resummed prediction over to the fixed-order prediction more quickly as y_{cut} increases, and might therefore be more reliable at large y_{cut}, but we have not yet implemented it. One could try to define an analog of $\ln R$ matching by

$$R_4^{\ln R\text{ match}} = R_4^{\text{NLL}} \frac{B_4}{B_4^{\text{NLL}}} \exp\left[\frac{\alpha_s}{2\pi}\left(-2 + \frac{C_4}{B_4} - \frac{C_4^{\text{NLL}}}{B_4^{\text{NLL}}}\right)\right], \tag{17}$$

but B_4^{NLL} vanishes for $y_{\text{cut}} \sim 0.01$, so this approach fails.

We evaluate the resummed R_4^{NLL} using the two-loop formula (12) for the running coupling appearing in Eq. (14). To evaluate the renormalization-scale dependence of R_4^{NLL} we make the substitution $\alpha_s \to \alpha_s + \beta_0 \ln(\mu^2/s)\alpha_s^2/2\pi$. In Fig. 4 we show the resummed and matched prediction $R_4^{R\text{ match}}$ for the Durham algorithm, together with the tree-level and one-loop fixed-order predictions. In order to illustrate once more that the subleading-color terms are small we also show the leading-color one-loop result in Fig. 4.
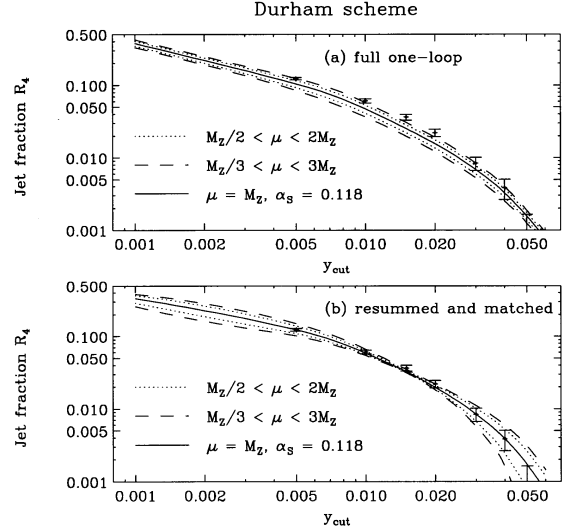

FIG. 5. Dependence on the renormalization scale of (a) the full one-loop prediction and (b) the resummed and matched result, for the Durham algorithm at $\sqrt{s} = M_Z$.

The agreement between theory and data is spectacularly good for the resummed and matched prediction. On the other hand, the ''scale uncertainty'' in the prediction is still sizable. This is illustrated in Fig. 5 where the full one-loop and the resummed and matched results are shown as bands. These bands have been obtained by varying the renormalization scale from $\frac{1}{2}M_Z < \mu < 2M_Z$ and $\frac{1}{3}M_Z < \mu < 3M_Z$, respectively. (The large scale dependence at large y_{cut} in the resummed and matched prediction might be improved by a modified matching scheme.)

V. CONCLUSIONS

In this work we presented the complete $O(\alpha_s^3)$ results for four-jet production in electron-positron annihilation. Generally, the NLO corrections are large and improve the agreement between theory and experiment considerably. The $1/N_c^2$-suppressed correction terms are indeed smaller than the leading-color terms by the naive factor of 10 or so. For the Durham algorithm, after the large logarithms of $1/y_{\text{cut}}$ have been resummed and the result is matched to the fixed-order prediction, and evaluated at the renormalization scale $\mu = \sqrt{s}$, theory agrees remarkably well with Z^0 data. Because the NLO corrections to the overall rate are so large, significant renormalization-scale dependence remains for both the fixed-order and resummed predictions, suggesting that there are still ~ 10–20% uncertainties from uncalculated higher-order corrections. More precise NLO predictions are possible for normalized four-jet distributions, for example the angles defined in [12], and will be reported elsewhere [17].

Note added in proof. After we submitted this manuscript, Campbell, Glover, and Miller reported on an independent calculation of the type (I) contributions to the one-loop virtual matrix elements for $e^+e^- \to q\bar{q}gg$ [32]. We have subsequently compared the virtual matrix elements used in this paper [9,10] to the results of [32,8] and we find agreement for both the four-quark and the two-quark–two-gluon final states. We thank J. M. Campbell and E. W. N. Glover for providing us with numerical results from [32,8]. Also, Nagy

and Trócsányi [33] have recently repeated our NLO calculation of R_4 for the Durham, Geneva, and E0 algorithms, using the matrix elements of [32,8]. They obtain general agreement with our results, within statistical uncertainties. However, a relatively large difference (compared to the statistical errors) occurring at large y_{cut} for the Geneva algorithm needs further investigation.

[1] Z. Kunszt and P. Nason, in *Z Physics at LEP 1*, Proceedings of the Workshop, Geneva, Switzerland, 1989, edited by G. Altarelli *et al.* (CERN Yellow Report No. 89-08, Geneva, 1989); G. Kramer and B. Lampe, Z. Phys. C **34**, 497 (1989); **42**, 504(E) (1989); Fortschr. Phys. **37**, 161 (1989); W.T. Giele and E.W.N. Glover, Phys. Rev. D **46**, 1980 (1992); S. Catani and M.H. Seymour, Phys. Lett. B **378**, 287 (1996); Z. Nagy and Z. Trócsányi, Nucl. Phys. **B486**, 189 (1997).

[2] OPAL Collaboration, P.D. Acton *et al.*, Z. Phys. C **55**, 1 (1992); L3 Collaboration, O. Adriani *et al.*, Phys. Lett. B **284**, 471 (1992); DELPHI Collaboration, P. Abreu *et al.*, Z. Phys. C **59**, 21 (1993); SLD Collaboration, K. Abe *et al.*, Phys. Rev. D **51**, 962 (1995).

[3] OPAL Collaboration, P.D. Acton *et al.*, Z. Phys. C **59**, 1 (1993): ALEPH Collaboration, D. Decamp *et al.*, Phys. Lett. B **284**, 163 (1992).

[4] A. Signer and L. Dixon, Phys. Rev. Lett. **78**, 811 (1997).

[5] A. Signer, Comput. Phys. Commun. (to be published).

[6] F.A. Berends, W.T. Giele, and H. Kuijf, Nucl. Phys. **B321**, 39 (1989).

[7] K. Hagiwara and D. Zeppenfeld, Nucl. Phys. **B313**, 560 (1989); N.K. Falck, D. Graudenz, and G. Kramer, *ibid.* **B328**, 317 (1989).

[8] E.W.N. Glover and D.J. Miller, Phys. Lett. B **396**, 257 (1997).

[9] Z. Bern, L. Dixon, D.A. Kosower, and S. Weinzierl, Nucl. Phys. **B489**, 3 (1997).

[10] Z. Bern, L. Dixon, and D.A. Kosower, in *QCD and QED in Higher Orders*, Proceedings of the Zeuthen Workshop, Rheinsberg, Germany, 1996, edited by J. Blumlein *et al.* [Nucl. Phys. B (Proc. Suppl.) **51C**, 243 (1996)]; e-print hep-ph/9708239.

[11] S. Catani, Yu.L. Dokshitser, M. Olsson, G. Turnock, and B.R. Webber, Phys. Lett. B **269**, 432 (1991).

[12] J.G. Körner, G. Schierholz, and J. Willrodt, Nucl. Phys. **B185**, 365 (1981); O. Nachtmann and A. Reiter, Z. Phys. C **16**, 45 (1982); M. Bengtsson and P.M. Zerwas, Phys. Lett. B **208**, 306 (1988); M. Bengtsson, Z. Phys. C **42**, 75 (1989).

[13] G.R. Farrar, Phys. Lett. B **265**, 395 (1991); Phys. Rev. D **51**, 3904 (1995); J. Ellis, D. Nanopoulos, and D. Ross, Phys. Lett. B **305**, 375 (1993); R. Muñoz-Tapia and W.J. Stirling, Phys. Rev. D **49**, 3763 (1994); **52**, 3894 (1995); F. Cuypers, *ibid.* **49**, 3075 (1994); S. Moretti, R. Muñoz-Tapia, and K. Odagiri, Phys. Lett. B **389**, 545 (1996); e-print hep-ph/9609295.

[14] A. de Gouvea and H. Murayama, Phys. Lett. B **400**, 117 (1997).

[15] OPAL Collaboration, R. Akers *et al.*, Z. Phys. C **65**, 367 (1995); **67**, 203 (1995).

[16] ALEPH Collaboration, R. Barate *et al.*, CERN Report No. CERN-PPE/97-002 (unpublished).

[17] A. Signer and L. Dixon (in preparation).

[18] S. Bethke, Z. Kunszt, D.E. Soper, and W.J. Stirling, Nucl. Phys. **B370**, 310 (1992).

[19] SLD Collaboration, K. Abe *et al.*, Phys. Rev. Lett. **71**, 2528 (1993); SLD Collaboration, P. Burrows (private communication).

[20] R.K. Ellis, D.A. Ross, and A.E. Terrano, Phys. Rev. Lett. **45**, 1226 (1980); Nucl. Phys. **B178**, 421 (1981).

[21] B. Kniehl and J. H. Kühn, Phys. Lett. B **224**, 229 (1989); K. Hagiwara, T. Kuruma, and Y. Yamada, Nucl. Phys. **B358**, 80 (1991).

[22] G.P. Lepage, J. Comput. Phys. **27**, 192 (1978); Report No. CLNS-80/447, 1980 (unpublished).

[23] S. Frixione, Z. Kunszt, and A. Signer, Nucl. Phys. **B467**, 399 (1996).

[24] J.M. Campbell, E.W.N. Glover, and D.J. Miller, Nucl. Phys. **B498**, 397 (1997).

[25] Particle Data Group, R.M. Barnett *et al.*, Phys. Rev. D **54**, 1 (1996).

[26] N. Brown and W.J. Stirling, Z. Phys. C **53**, 629 (1992).

[27] K.G. Chetyrkin, Phys. Lett. B **391**, 402 (1997); L.J. Clavelli and L.R. Surguladze, Phys. Rev. Lett. **78**, 1632 (1997).

[28] F. Csikor and Z. Fodor, Phys. Rev. Lett. **78**, 1632 (1997).

[29] L3 Collaboration, B. Adeva *et al.*, Phys. Lett. B **248**, 227 (1990); DELPHI Collaboration, P. Abreu *et al.*, Z. Phys. C **59**, 357 (1993).

[30] R.K. Ellis, W.J. Stirling, and B.R. Webber, *QCD and Collider Physics* (Cambridge University Press, Cambridge, England, 1996).

[31] S. Catani, L. Trentadue, G. Turnock, and B.R. Webber, Nucl. Phys. **B407**, 3 (1993).

[32] J. M. Campbell, E. W. N. Glover, and D. J. Miller, hep-ph/9706297.

[33] Z. Nagy and Z. Trócsányi, hep-ph/9707309.